Carbon Nanotube Core–Polymer Shell Nanofibers

Jing Liu,[1] Tong Wang,[1] Tetsuya Uchida,[2] Satish Kumar[1]

[1]*School of Polymer, Textile and Fiber Engineering, Georgia Institute of Technology, Atlanta, Georgia 30332*
[2]*Faculty of Engineering, Okayama University, Okayama 700-8530, Japan*

Received 28 September 2004; accepted 3 October 2004
DOI 10.1002/app.21662
Published online in Wiley InterScience (www.interscience.wiley.com).

ABSTRACT: Single-walled carbon nanotube (SWNT)/poly(methyl methacrylate) and SWNT/polyacrylonitrile composite nanofibers were electrospun with SWNT bundles as the cores and the polymers as the shells. This was a novel approach for processing core (carbon nanotube)–shell (polymer) nanofibers. Raman spectroscopy results show strain-induced intensity variations in the SWNT radial breathing mode and an upshift in the tangential (*G*) and overtone of the disorder (*G′*) bands, suggesting compressive forces on the SWNTs in the electrospun composite fibers. Such fibers may find applications as conducting nanowires and as atomic force microscopy tips. © 2005 Wiley Periodicals, Inc. J Appl Polym Sci 96: 1992–1995, 2005

Key words: nanocomposites; atomic force microscopy (AFM); core-shell polymers; Raman spectroscopy; nanotube

INTRODUCTION

The incorporation of only a few percentage points of single-walled carbon nanotubes (SWNTs) into many polymers has led to a significant improvement in mechanical[1–3] and electrical[4] properties. To fully explore their reinforcing potential, a uniform SWNT dispersion, exfoliation, and orientation[5] are important. SWNTs have shown great potential as high-resolution atomic force microscopy (AFM) imaging probes[6] due to their small diameter, good mechanical properties, potential for chemical functionalization, and high electrical and thermal conductivities. Higher lateral resolution (better than 1 nm) and consistently and significantly better AFM image quality have been reported with nanotube tips than with the best silicon AFM tips.[7] There are several methods for attaching nanotubes to silicon AFM tips, including manual assembly,[8] direct growth,[9] and pickup.[10] Recently, the plasma-assisted deposition and polymerization of fluorocarbon polymers on the nanotubes for AFM tip application has been reported.[11] Electrospinning is an active area of research for the processing of nanofibers[12,13] and has been explored in more than 30 polymers, including polyacrylonitrile (PAN),[14] poly(vinyl alcohol),[15] nylon 6,[16] and poly(ethylene oxide).[17] The incorporation of carbon nanotubes into electrospun nanofibers results in improved mechanical properties and electrical conductivity.[18] In this article, we report the electrospinning of core (SWNT bundle)–shell (polymer) nanocomposite fibers. These core–shell fibers should have applications as AFM tips and in other nanodevices. Polymer–SWNT interaction in the electrospun fibers was studied with Raman spectroscopy.

EXPERIMENTAL

Purified HiPCO SWNTs (containing 10 wt % catalyst based on thermogravimetric analysis) were obtained from Carbon Nanotechnologies, Inc. (Houston, TX). Poly(methyl methacrylate) [PMMA; weight-average molecular weight (M_w) = 95,000–150,000 g/mol] was obtained from Cyro Industries (Osceola, AR). PAN (M_w = 100,000 g/mol) was obtained from Japan Exlan Co. Ltd (Osaka, Japan) and nitromethane and *N*,*N*-dimethylformamide were obtained from Aldrich (Milwaukee, WI). All materials were used as received. The SWNTs (10 mg) were dispersed in 200 mL of solvent (nitromethane for PMMA and *N*,*N*-dimethylformamide for PAN) by sonication (Branson water bath sonicator by Smithkline Co. (Philadelphia, PA), model B-22-4, power = 125 W, frequency = 43 KHz) for 48 h at room temperature. PMMA or PAN was added to this dispersion, and the mixture was then stirred for 10 h at 700 rpm. The optically homogeneous polymer–SWNT–solvent dispersion was also poured onto a glass plate, the solvent was allowed to evaporate in the hood over several days, and the film was peeled off of the plate. This film was designated as film A. A syringe pump (Fisher Scientific, Pittsburgh, PA), at a

Correspondence to: S. Kumar (satish.kumar@ptfe.gatech.edu).

Contract grant sponsor: Office of Naval Research; contract grant number: N00014-01-1-0657.
Contract grant sponsor: Air Force Office of Scientific Research; contract grant number: F49620-03-1-0124.
Contract grant sponsor: Carbon Nanotechnologies, Inc.

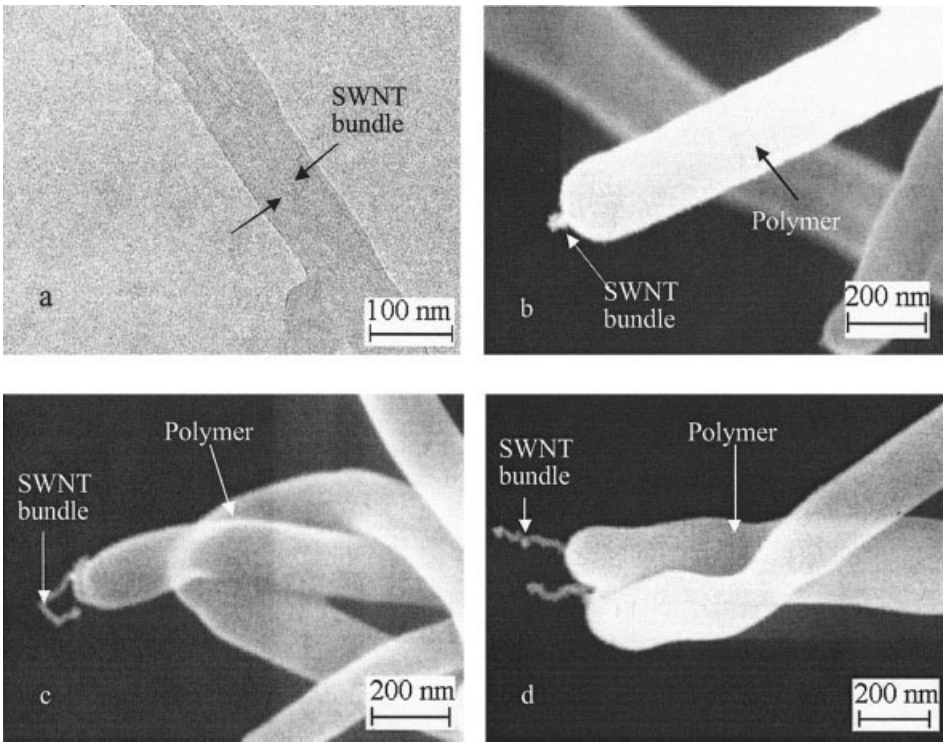

Figure 1 (a) High-resolution transmission electron micrograph of the electrospun PAN/SWNT composite fiber and (b, c, and d) scanning electron micrographs of electrospun SWNT/PMMA fibers.

flow rate of 1 mL/h, was used for electrospinning at 22 kV, whereas the collection target (a grounded steel sheet) was placed at a distance of 10 cm from the syringe needle. The electrospun fiber mat was simply designated as the fiber mat. This fiber mat was heated in a differential scanning calorimeter (TA Instruments, New Castle, DE) from 25 to 150°C at 10°C/min and then cooled at the same rate to room temperature to relax any thermal strains in the sample. The sample treated by differential scanning calorimetry was designated as film B. Scanning electron microscopy (LEO 1530; Oberkochen, Germany) was done on gold-coated samples. A JEM 2000EX (200 kV) (Tokyo, Japan) instrument was used for high-resolution transmission electron microscopy. Raman spectroscopy was done on a Holoprobe Raman microscope from Kaiser Optical Systems, Inc. (Ann Arbor, MI), with a 785-nm excitation wavelength [laser excitation energy (E_{laser}) = 1.58 eV].

RESULTS AND DISCUSSION

SWNT/PAN and SWNT/PMMA composite fibers containing SWNT bundles as the core were processed by electrospinning (Fig. 1). SWNT bundles (20–30 nm in diameter) were aligned along the fiber axis, as shown by the high-resolution transmission electron micrograph [Fig. 1(a)]. Scanning electron micrographs of the SWNT/PMMA fibers showed a SWNT bundle protruding at the end of the composite fiber. Some buckling[10,19] was observed in the protruded SWNT bundles, and buckling was minimized when the SWNT tail was short [Fig. 1(b)]. Fibers with a sheath–core structure can be used as electrically conductive nanowires and as nanoelectrodes in electrochemical devices where the nanotube core is used for conduction and the shell polymer is used as an insulator. Another important application is AFM probe tips, where the individual SWNT or small SWNT bundles can be used to achieve high resolution, whereas the larger diameter shell provides rigidity and ease of handling. The core diameter is the diameter of the individual nanotube or that of the nanotube bundle, depending on the extent of exfoliation. Highly exfoliated systems, such as poly(vinyl alcohol)/poly(2-vinylpyridine)/sodium dodecyl sulfate/SWNT,[20] can be electrospun into nanofibers with different size nantoube AFM tips. One can tailor the tip length by etching the polymer with an electron beam, as the electron beam resistivity of the carbon nanotubes is about five orders of magnitude higher than the flexible chain polymers such as poly(vinyl alcohol), poly(ethylene oxide), polyethylene, and PMMA. Electrospinning can also be done on the functionalized nanotube–polymer composites. Use of chemically or biologically functionalized tips, as well tips with electrical and thermal conductivity provides additional capability to the atomic force microscope. The electrospun fibers can typically be processed in the 100 nm to 2 μm diameter range by the control of solution characteris-

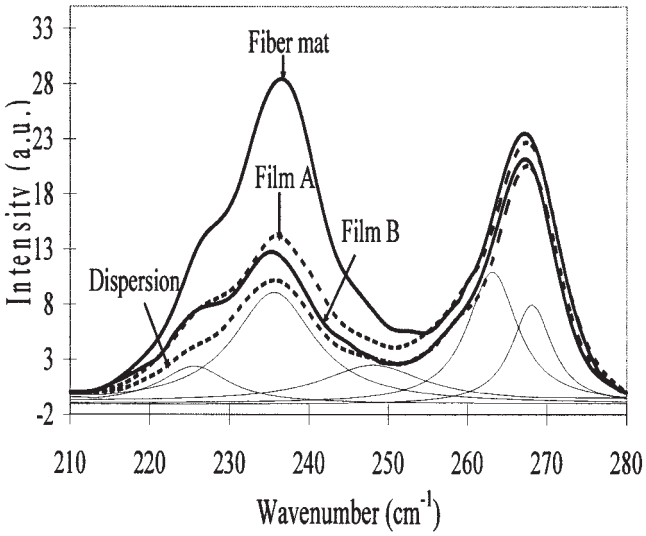

Figure 2 Raman RBM spectra of PMMA/SWNT samples containing 1 wt % SWNT, with respect to the weight of PMMA.

tics (type of polymer, solution concentration, and polarity and surface tension of the solvent) and processing parameters (strength of the applied electric field, distance between the spinneret and collector, and solution feeding rate). Electrospinning can be used to process continuous core (nanotube)–shell (polymer) fibers with a large number[12,13] of polymers.

Raman spectroscopy is a powerful and nondestructive method for characterizing SWNT and its interaction with other molecules and the effect of pressure[21] and temperature.[22] According to resonance theory, the intensity of the Raman bands depends on the difference between E_{laser} and the van Hove transition energy (E_{ii}). Raman radial breathing mode (RBM) intensity increases when the difference $|E_{ii} - E_{laser}|$ decreases and vice versa and reaches a maximum value when $E_{ii} = E_{laser}$. The Raman RBM spectra of the SWNT/PMMA composites (Fig. 2) were been fitted with five Lorentzian components located at 226, 236, 248, 263, and 268 cm^{-1}, and the fitted results of film A are shown in Figure 2 as an example. When[23] tube diameter (d_t) (nm) = $223.5/[\omega_{RBM}\ (cm^{-1}) - 12.5]$ for the SWNT bundle, individual nanotube diameters in the 0.88 nm to 1.05 nm range were obtained. Here ω_{RBM} is the radial breathing mode frequency in wave number. Only semiconducting tubes were seen in RBM mode with a 785 nm wavelength laser, and the metallic tubes required a different excitation energy. The RBM intensities of the various samples shown in Figure 2 were normalized to the tangential (G) band intensity. After this normalization, the area of the peak at 265 cm^{-1} (composite of 263 and 268-cm^{-1} peaks) was almost the same for the four samples for which data is shown in Figure 2. Similar to the treatment of Lucas and Young,[24] under compressive strain, the second order van Hove transition for the semi-conducting tube (E^s_{22}) increased for the tube corresponding to the 263 cm^{-1} RBM peak and decreased for the tube corresponding to the 268-cm^{-1} peak.[25] The E^s_{22} values for both of these tubes (1.8–1.90 eV) were quite far from the E_{laser} values. Thus, the other peak areas could also be normalized with respect to the 265-cm^{-1} peak. E^s_{22} of the 236-cm^{-1} band was reported[26] to be between 1.59 and 1.67 eV. Under compressive strain, it decreased and approached closer to the E_{laser} (1.58 eV) value. Therefore, the intensity of the 236-cm^{-1} band increased under compression. The 236-cm^{-1} band intensities of film A, film B, and the dispersion were quite comparable, whereas the intensity of the electrospun fiber mat was much higher. This suggests that in the electrospun fiber, the nanotubes experienced higher compressive strains than in the other three samples. Corresponding shifts were also observed in the positions of the tangential (G) and overtone of the disorder (G') Raman bands (Fig. 3), as shown by the linear relationship between the 236-cm^{-1} band intensity and the G and G' band peak positions.

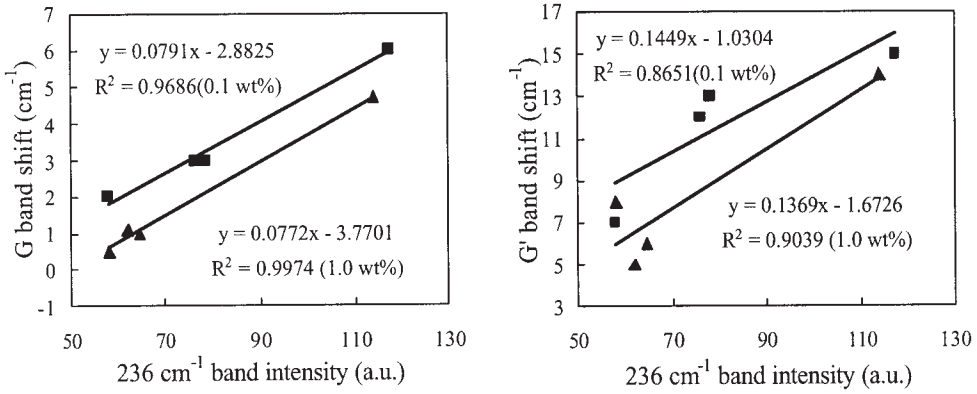

Figure 3 Raman G and G' band shifts as a function of 236-cm^{-1} band intensity in the PMMA/SWNT composites: (■) 0.1 wt % SWNT and (▲) 1.0 wt % SWNT in PMMA. The samples from low to high 236-cm^{-1} band intensity (or from low to high G and G' shifts) were dispersion, film B, film A, and the electrospun fiber mat.

CONCLUSIONS

SWNT/PMMA and SWNT/PAN composite fibers hundreds of nanometers in diameter containing SWNT bundles as the core were processed by electrospinning. This is a general method and can be used with a large number of polymers. Although in this experiment, we showed the core to be a SWNT bundle, once the SWNTs were fully exfoliated, an individual nanotube could form the core of these fibers. Such fibers are expected to find applications in nanodevices and as AFM tips. Nanotubes in the electrospun fibers experienced compressive strain, which resulted in the enhanced intensity of the selected Raman RBM peak and an upshift in the *G* and *G′* band positions.

References

1. Sreekumar, T. V.; Liu, T.; Min, B. G.; Guo, H.; Kumar, S.; Hauge, R. H.; Smalley, R. E. Adv Mater 2004, 16, 58.
2. Kumar, S.; Dang, T. D.; Arnold, F. E.; Bhattacharyya, A. R.; Min, B. G.; Zhang, X.; Vaia, R. A.; Park, C.; Adams, W. W.; Hauge, R. H.; Smalley, R. E.; Ramesh, S.; Willis, P. A. Macromolecules 2002, 35, 9039.
3. Sen, R.; Zhao, B.; Perea, D.; Itkis, M. E.; Hu, H.; Love, J.; Bekyarova, E.; Haddon, R. C. Nano Lett 2004, 4, 459.
4. Benoit, J. M.; Corraze, B.; Lefrant, S.; Blau, W. J.; Bernier, P.; Chauvet, O. Synth Met 2001, 121, 1215.
5. Liu, T.; Kumar, S. Nano Lett 2003, 3, 647.
6. Wong, S. S.; Woolley, A. T.; Odom, T. W.; Huang, J. L.; Kim, P.; Vezenov, D. V.; Lieber, C. M. Appl Phys Lett 1998, 73, 3465.
7. Wade, L. A.; Shapiro, I. R.; Ma, Z.; Quake, S. R.; Collier, C. P. Nano Lett 2004, 4, 725.
8. Dai, H.; Hafner, J. H.; Rinzler, A. G.; Colbert, D. T.; Smalley, R. E. Nature 1996, 384, 147.
9. Hafner, J. H.; Cheung, C.-L.; Lieber, C. M. Nature 1999, 398, 761.
10. Hafner, J. H.; Cheung, C.-L.; Oosterkamp, T. H.; Lieber, C. M. J Phys Chem B 2001, 105, 743.
11. Esplandiu, M. J.; Bittner, V. G.; Giapis, K. P.; Collier, C. P. Nano Lett 2004, 4, 1873.
12. Dzenis, Y. Science 2004, 304, 1917.
13. Li, D.; Xia, Y. Adv Mater 2004, 16, 1151.
14. Kim, C.; Yang, K. S. Appl Phys Lett 2003, 83, 1216.
15. Shao, C.; Kim, H.-Y.; Gong, J.; Ding, B.; Lee, D.-R.; Park, S.-J. Mater Lett 2003, 57, 1579.
16. Fong, H.; Liu, W.; Wang, C.-S.; Vaia, R. A. Polymer 2002, 43,775.
17. Fong, H.; Chun, I.; Reneker, D. H. Polymer 1999, 40, 4585.
18. Seoul, C.; Kim, Y.-T.; Baek, C.-K. J Polym Sci Part B: Polym Phys 2003, 41, 1572
19. Dai, H.; Hafner, J. H.; Rinzler, A. G.; Colbert, D. T.; Smalley, R. E. Nature 1996, 384, 147.
20. Zhang, X.; Liu, T.; Sreekumar, T. V.; Kumar, S.; Moore, V. C.; Hauge, R. H.; Smalley, R. E. Nano Lett 2003, 3 1285.
21. Dharap, P.; Li, Z.; Nagarajaiah, S.; Barrera, E. V. Nanotechnology 2004, 15, 379.
22. Huang, F.; Yue, K.; Tan, P.; Zhang, S.; Shi, Z.; Zhou, X.; Gu, Z. J Appl Phys 1998, 84, 4022.
23. Bachilo, S. M.; Strano, M. S.; Kittrell, C.; Hauge, R. H.; Smalley, R. E.; Weisman, R. B. Science 2002, 298, 2361.
24. Lucas, M.; Young, R. J. Phys Rev B 2004, 69, 85405.
25. Liu, J.; Liu, T; Kumar, S. Polymer 2005, in press.
26. Dresselhaus, M. S.; Eklund, P. C. Adv Phys 2000, 49, 705.